CD-aware non-orthogonal DFT-precoding for C-band IM/DD multicarrier signals over a 50-km dispersion-uncompensated link

Junwei Zhang, 1,2,* $^{\bullet}$ Liwang Lu, 2 Heyun Tan, 1 Alan Pak Tao Lau, 2 and Chao Lu 1,2

¹School of Electronics and Information Technology, Sun Yat-sen University, Guangzhou 510275, China ²Photonics Research Institute, Department of Electrical and Electronic Engineering, The Hong Kong Polytechnic University, Hong Kong SAR, China *zhangjw253@mail.sysu.edu.cn

Abstract: In this paper, a chromatic-dispersion-aware non-orthogonal discrete Fourier transform precoding (CDA-NODFTP) scheme is proposed for CD-constrained intensity-modulation and direct detection (IM/DD) multicarrier-signal transmission systems. The performance of the proposed CDA-NODFTP scheme is experimentally evaluated and compared with conventional DFTP and NODFTP schemes over a 50-km C-band dispersion-uncompensated link, utilizing 90-Gb/s orthogonal frequency division multiplexing (OFDM) and filter bank multicarrier (FBMC) signals. Experimental results show that the proposed CDA-NODFTP with adaptive spectral compression outperforms conventional DFTP, NODFTP, and the non-precoding schemes in terms of bit error rate (BER) performance. Moreover, based on CD response only, the CDA-NODFTP-FBMC exhibits superior performance compared to both CDA-NODFTP-OFDM and adaptive bit and power loading (ABPL) FBMC, achieving receiver sensitivity improvements of over 2 dB at a BER of 3.8×10^{-3} .

© 2024 Optica Publishing Group under the terms of the Optica Open Access Publishing Agreement

1. Introduction

To support the exponential growth of data traffic in optical data-center interconnections and access networks, while simultaneously meeting the strict requirements for low-cost, high energy efficiency, and small form factors, intensity modulation and direct detection (IM/DD) optical transmission employing double-sideband (DSB) modulation is regarded as a promising solution [1,2]. The interaction between chromatic dispersion (CD) and square-law detection, however, introduces significant frequency-selective power fading on C-band optical DSB signals over long fiber distances [2-4]. This leads to the presence of spectral nulls and a non-uniform frequency response, thereby causing a substantial degradation in the performance of IM/DD systems. The IM/DD orthogonal frequency division multiplexing (OFDM) [4] and filter bank multicarrier (FBMC) [5] techniques are two widely adopted solutions for effectively minimize the impact of CD-induced power fading by fully leveraging the channel characteristics through an adaptive bit and power loading algorithm. Compared with OFDM system, the FBMC system with a well-localized prototype filter in both time and frequency domains exhibits stronger robustness against CD-induced power fading even without employing a cyclic prefix (CP), thereby resulting in an improved system capacity [5]. Nevertheless, the implementation of adaptive bit and power loading necessitates an additional reverse link for precise feedback of channel state information (CSI), generally the signal-to-noise ratio (SNR), over all data-carrying subcarriers [6]. To avoid the feedback of CSI, various channel-independent precoding techniques such as discrete Fourier transform (DFT) precoding, orthogonal circulant transform (OCT) precoding, constant amplitude zero autocorrelation (CAZAC), and Walsh-Hadamard transform (WHT) have been widely investigated for IM/DD OFDM and FBMC systems to equalize non-uniform SNR

#523497 Journal © 2024 https://doi.org/10.1364/OE.523497

Received 11 Mar 2024; revised 7 Jun 2024; accepted 24 Jun 2024; published 8 Jul 2024

and bit error rate (BER) responses caused by bandwidth limitations [7,8]. Recently, a novel non-orthogonal DFT-precoding based OFDM (NODFTP-OFDM) technique [9,10], also named as DFT-spread spectrally efficient frequency division multiplexing (DFTS-SEFDM) [11], was proposed to enhance robustness against the steep frequency roll-off in either the low-frequency or high-frequency region through effective bandwidth compression. Different from conventional SEFDM [12,13], the NODFTP-OFDM features the advantages of low peak-to-average power ratio (PAPR) and high compatibility with advanced digital signal processing (DSP) techniques already employed in OFDM, such as simple one-tap frequency-domain equalization (FDE) [9–11]. However, the effectiveness of the abovementioned channel-independent precoding techniques would be limited in CD-constrained IM/DD systems that experience severe CD-induced power fading.

In this paper, we propose a CD-aware NODFTP (CDA-NODFTP) scheme to enhance resistance against CD-induced power fading in a C-band IM/DD multicarrier-signal transmission system. Based on the prior knowledge of the dispersive channel, the CDA-NODFTP can flexibly keep the multicarrier signals' electrical spectra away from the CD-induced spectral nulls without sacrificing spectral efficiency (SE). The inter-carrier interference (ICI) induced by CDA-NODFTP is mitigated using a cascaded binary-phase-shift-keying iterative detection (CBID) algorithm [13]. The performance of the proposed CDA-NODFTP scheme is evaluated in a C-band 90-Gb/s IM/DD transmission system employing OFDM and FBMC signals over a 50-km dispersionuncompensated link. The BERs of multicarrier signals, both with and without DFTP/NODFTP, are above 0.03 due to the severe CD-induced power fading, making them unsuitable for supporting data transmission at a rate of 90 Gb/s. While the proposed CDA-NODFTP significantly reduces the BERs of OFDM and FBMC signals, achieving reductions in BER by approximately one and two orders of magnitude, respectively. When compared to CDA-NODFTP-OFDM, utilizing a well-localized prototype filter in both time and frequency domains enables CDA-NODFTP-FBMC to achieve a more than 3-dB improvement in receiver sensitivity, at the 7% hard-decision forward error correction (HD-FEC) BER limit of 3.8×10^{-3} . Meanwhile, the CDA-NODFTP-FBMC exhibits superior performance compared to adaptive bit and power loading (ABPL) FBMC using CD response only, resulting in an approximately 2.1-dB improvement in receiver sensitivity. These results highlight the potential of implementing CDA-NODFTP scheme in high-speed optical IM/DD multicarrier transmission systems, particularly for FBMC system.

2. Principle and decoding of CD-aware non-orthogonal DFT precoding

Principle of CD-aware non-orthogonal DFT precoding for IM/DD multicarrier signals

The conventional DFTP scheme, as illustrated in Fig. 1(a), employs N-point DFT to perform precoding for N quadrature amplitude modulation (QAM) symbols. The subcarrier mapping (allocated to the $2^{\rm nd} - (N+1)^{\rm th}$ subcarriers) and Hermitian symmetry are subsequently applied prior to converting the precoded symbols into a real-valued OFDM symbol in the time domain using a $N_{\rm fft}$ -point ($N_{\rm fft} \geq 2(N+1)$) inverse DFT (IDFT). Noted that the FBMC requires an additional operation of offset QAM (OQAM) modulation [5], as opposed to OFDM, before converting from the frequency domain to the time domain. The original transmitted symbols can be recovered at the receiver by performing N-point IDFT over N data-carrying subcarriers.

However, in the presence of severe CD-induced power fading in the IM/DD transmission system, the precoding performance is significantly degraded due to a substantial number of spectral nulls within the signal bandwidth, thereby making it ineffective. Here the proposed CDA-NODFTP scheme is designed to overcome this limitation without sacrificing SE, by leveraging prior knowledge of the normalized power response of the SSMF channel given by $P(f) = \cos^2(2\pi^2\beta_2 L f^2)$, where $\beta_2 = -D\lambda^2/(2\pi c)$ is the group velocity dispersion (GVD) of SSMF, with λ , c, and D denoting the wavelength, speed of light, and dispersion coefficient,

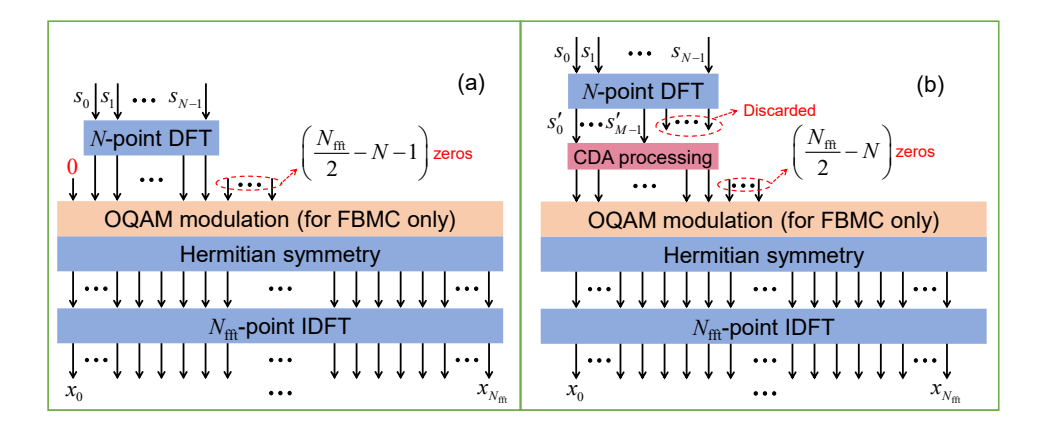


Fig. 1. Principles of (a) conventional DFTP and (b) CDA-NODFTP for multicarrier signals.

respectively. The principle of the proposed CDA-NODFTP, which aims to enhance resistance against CD-induced power fading and keep SE unchanged, is depicted in Fig. 1(b) and summarized as follows: (1) Retain the first M data samples of the output of a N-point DFT, and discard the remaining (N-M) data samples. (2) Calculate the power response $P(f_n) = P(nf_s/N_{\rm fit})$ for subcarriers with subcarrier indexes of $n=1,\cdots N-1$, where f_s represents the sampling rate. (3) Perform the CDA processing, in which only M out of (N-1) subcarriers with higher calculated power responses are selected to transmit the retained M data samples, while setting the data values of the first subcarrier (subcarrier index of n=0) and other subcarriers to 0. After conducting CDA processing, subcarrier mapping (allocated to the $1^{\rm st}-N^{\rm th}$ subcarriers) and Hermitian symmetry are applied before performing $N_{\rm fit}$ -point ($N_{\rm fit} \geq 2N$) IDFT. Consequently, the signal bandwidth is adaptively compressed to keep away from the direct current (DC) and spectral nulls, with the compression factor defined as $\alpha = M/N$.

2.2. Decoding of CD-aware non-orthogonal DFT precoding for IM/DD multicarrier signals

The decoding process at the receiver involves padding N-M zeros for the corresponding subcarriers of the discarded samples in the frequency domain after extracting M data subcarriers, followed by applying a N-point IDFT [11]. The orthogonality between the $N_{\rm fit}$ -point IDFT and DFT is maintained since compression is performed prior to the $N_{\rm fit}$ -point IDFT, while nonorthogonality only exists between the N-point DFT and IDFT. Thus, the decoded symbols suffer from ICI caused by spectral compression. This ICI can be mitigated using a CBID algorithm [13] based on the $N \times N$ correlation matrix C, where its $(k, i)^{\rm th}$ entry is given by

$$C_{k,i} = \frac{1}{N} \sum_{n=0}^{M} \exp\left(\frac{j2\pi n(k-i)}{N}\right)$$
 (1)

Obviously, the identity matrix C is obtained when M equals N, indicating the absence of ICI in conventional DFTP. The symbol vector \mathbf{Y}_g , recovered after ICI mitigation in the g^{th} iteration of CBID, can be expressed as [13]

$$\mathbf{Y}_{\varrho} = \mathbf{R} + (\mathbf{I} - \mathbf{C})\mathbf{Y}_{\varrho - 1} \tag{2}$$

where **R** is the decoded symbol vector, **I** is the identity matrix, and \mathbf{Y}_{g-1} represents the recovered symbol vector after mitigating ICI in the $(g-1)^{\text{th}}$ iteration. The computational complexity of the CBID algorithm can be quantified by the number of complex-valued multiplications

per OFDM/FBMC symbol, which is GN^2 , given that a quadrature-phase-shift keying (QPSK) format is employed in this work, where G represents the total number of iterations. In the processes of non-orthogonal precoding and decoding, $2N^2$ complex-valued multiplications are required to execute N-point DFT and IDFT operations, which can be reduced to $N\log_2(N)$ with hardware-efficient radix-2 fast Fourier transform (FFT) when N is chosen to be a power of 2.

3. Experimental setup

The performance of the proposed CDA-NODFTP scheme is evaluated in a C-band 90-Gb/s IM/DD transmission system, employing OFDM and FBMC signals over a 50-km SSMF. Figure 2 illustrates the experimental setup and the DSP block diagram. The first step in OFDM generation involves the generation of a pseudo random bit sequence (PRBS), which is then mapped onto QPSK symbols. After performing QPSK mapping and serial-to-parallel (S/P) conversion, the parallel symbols allocated across 192 subcarriers (N = 192) are processed by the CDA-NODFTP. This processing includes a 192-point FFT, as well as a CDA module that compresses the resulting 192 samples into M samples. The subcarrier mapping (allocated to the $1^{st} - 192^{th}$ subcarriers) and Hermitian symmetry are applied prior to performing a 512-point FFT (IFFT) for generating a real-valued signal. After adding a 32-point cyclic prefix (CP), parallel-to-serial (P/S) conversion and hard clipping are carried out. In order to generate a CP-free FBMC signal, further steps involving OQAM modulation and pulse shaping using polyphase network (PPN) are performed [5]. The Mirabbasi-Martin filter with an overlapping factor K of 4 is utilized as the prototype filter in the PPN [14]. The distinction in signal generation between the OFDM and FBMC signals can be observed by utilizing yellow blocks in Fig. 2. The offline-generated OFDM or FBMC signal is fed into an arbitrary waveform generator (AWG, Keysight M8194A) at 120 GSa/s. The electrical signal from the AWG is amplified by an electrical amplifier (EA, SHF M807) prior to being applied to a Mach-Zehnder modulator (MZM, iXblue MXER-LN-10) operating at the quadrature point. The optical carrier is generated by an external cavity laser (ECL) operating at a wavelength of 1550.12 nm. After 50-km SSMF transmission, an Erbium-doped fiber amplifier (EDFA) is employed to boost the power up to 6 dBm. A variable optical attenuator

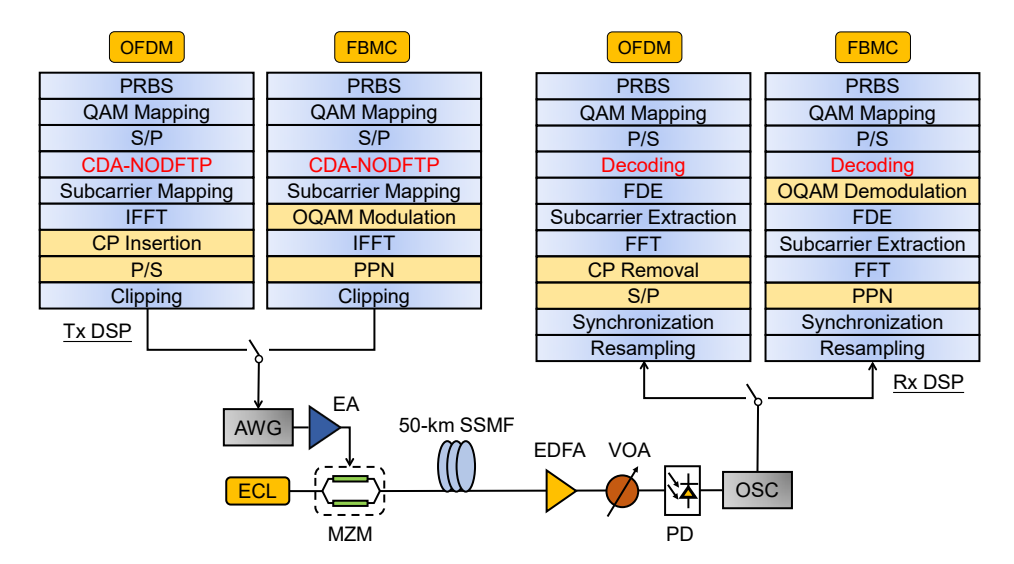


Fig. 2. Experimental setup and DSP block diagram. AWG: arbitrary waveform generator; EA: electrical amplifier; MZM: Mach-Zehnder modulator; ECL: external cavity laser; SSMF: standard single mode fiber; EDFA: erbium doped fiber amplifier; VOA: variable optical attenuator; PD: photodetector; OSC: real-time oscilloscope.

(VOA) is inserted for adjusting the received optical power (ROP) of the received signal, which is then detected by a 70-GHz photodetector (PD) without utilizing a trans-impedance amplifier (TIA). The detected signal is subsequently digitized and stored by a real-time oscilloscope (OSC, Keysight DSAZ594A) at 160 GSa/s. Finally, the offline OFDM DSPs perform a series of operations in reverse order compared to the transmitter side, including resampling to 120 GSa/s, timing synchronization, S/P conversion, CP removal, FFT, data subcarrier extraction, one-tap FDE, decoding, P/S conversion, QPSK demapping, and BER calculation. For FBMC system, additional DSPs are required for filtering with PPN and OQAM demodulation [5]. Except for one symbol dedicated to synchronization, each data frame consists of 900 QPSK symbols for each data subcarrier, in which the first 100 symbols serve as training symbols for channel estimation while the remaining symbols serve as effective data symbols.

4. Results and analysis

The frequency response characteristic of the SSMF channel is firstly investigated, followed by a comparison of the SNR performance between multicarrier signals with and without conventional DFTP. The frequency response of the back-to-back (BTB) system is depicted in Fig. 3(a), illustrating that the overall system exhibits a -15-dB bandwidth of approximately 45 GHz and a sharp roll-off above 45 GHz. Consequently, the experiment is conducted with a signal bandwidth of 45 GHz. The theoretical frequency response, calculated with a dispersion coefficient D of 16.75 ps/ns/km, is depicted in Fig. 3(b), alongside the electrical spectra of received OFDM and FBMC signals after 50-km SSMF transmission. It can be observed that the received signals suffer from severe CD-induced power fading, which aligns with the theoretical frequency response. The subcarrier-SNR distributions of conventional OFDM, FBMC, DFTP-OFDM, and DFTP-FBMC signals after 50-km SSMF transmission at a ROP of 6 dBm are illustrated in Fig. 3(c). The performance of both OFDM and FBMC is degraded due to the presence of numerous dips in the subcarrier-SNR distributions caused by severe CD-induced power fading. The well-localized prototype filter in FBMC allows for spectral overlap only between adjacent subcarriers, resulting in significant improvements in SNR compared to OFDM for the non-fading subcarriers as expected [5]. After implementing conventional DFTP, the subcarrier-SNR distributions of both OFDM and FBMC signals can be equalized to be relatively flat. However, owing to significant noise introduced within SNR dips caused by CD, all subcarrier-SNR values remain below 4 dB. Constrained by CD-induced power fading over a 50-km SSMF, the achievable BERs of conventional OFDM, FBMC, DFTP-OFDM and DFTP-FBMC signals at 90 Gb/s with QPSK format are 4.37×10^{-2} , 3.57×10^{-2} , 1.47×10^{-1} , and 1.15×10^{-1} at a ROP of 6 dBm, respectively, much higher than 3.8×10^{-3} of the 7% HD-FEC BER limit.

By leveraging CDA-NODFTP scheme to enhance resistance against CD-induced power fading, the transmission performance over a 50-km SSMF can be significantly enhanced. Figures 4(a) and 4(b) show the electrical spectra of transmitted and received CDA-NODFTP-OFDM and CDA-NODFTP-FBMC signals with M = 162 (corresponds a compression factor of 0.844), respectively. Thanks to the CDA processing, it is seen that the spectra of CDA-NODFTP-OFDM and CDA-NODFTP-FBMC signals are adaptively compressed to keep away from the spectral nulls caused by CD, while keeping SE unchanged. Moreover, by utilizing a well-localized prototype filter in both time and frequency domains, the CDA-NODFTP-FBMC features the advantage of lower out-of-band spectral/power leakage compared to CDA-NODFTP-OFDM.

The impact of the compression factor α on the BER performance with and without CBID algorithm is evaluated for 90-Gb/s CDA-NODFTP-OFDM and CDA-NODFTP-FBMC transmissions over a 50-km SSMF at a ROP of 6 dBm, as the results shown in Figs. 5(a) and 5(b), respectively. The number of iterations ν in the CBID algorithm is determined as 20 to ensure convergence. For comparison, the BER results of conventional DFTP, low-frequency compression based NODFTP (LFC-NODFTP) [9,10], high-frequency compression based NODFTP (HFC-NODFTP) [11] and

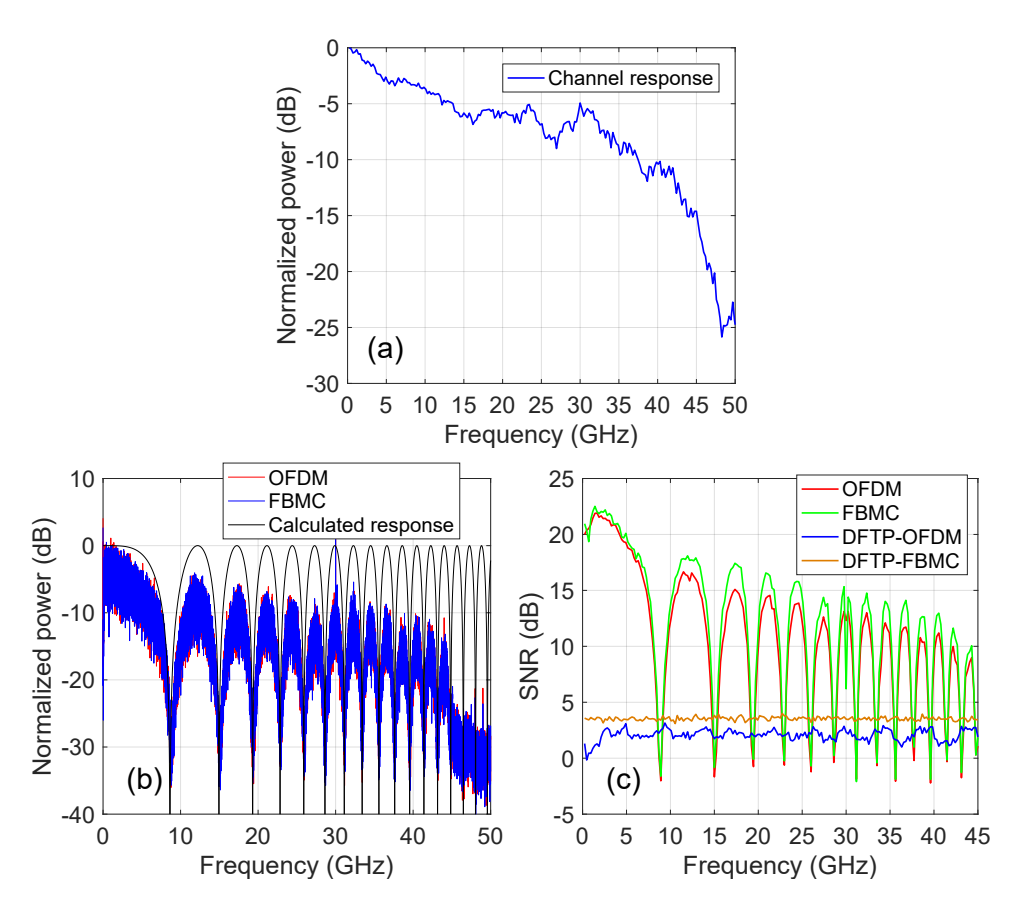


Fig. 3. (a) Normalized frequency response of the BTB system. (b) Calculated frequency response and electrical spectra of received electrical OFDM and FBMC signals after 50-km SSMF transmission. (c) Measured subcarrier-SNR distributions of a 50-km SSMF system using different signals.

the non-precoding counterparts are included in Figs. 5(a) and 5(b). The following observations can be made: (1) The BER performance of the CDA-NODFTP scheme first improves as the compression factor decreases, owing to the abandonment of subcarriers with low SNRs caused by CD-induced power fading. However, further reduction in compression factor leads to degradation in BER performance due to increased ICI. (2) Similar to conventional DFTP, the performance of NODFTP with low- or high-frequency bandwidth compression is severely degraded due to the dominant impairment caused by CD-induced spectral zeros, rather than bandwidth limitation in the low-frequency or high-frequency region. While the CDA-NODFTP scheme demonstrates superior BER performance compared to conventional schemes, both with and without the DFTP/NODFTP. (3) Thanks to ICI mitigation using the CBID algorithm, the optimal compression factors of CDA-NODFTP-OFDM and CDA-NODFTP-FBMC are significantly reduced to the same value of 0.844, which is notably lower than the value of 0.875 observed in the cases without CBID. (4) The proposed CDA-NODFTP with CBID effectively reduces the BERs of OFDM and FBMC signals by approximately one and two orders of magnitude, respectively. (5) The CDA-NODFTP-FBMC achieves better BER performance in comparison with CDA-NODFTP-OFDM, which can be attributed to its better robustness against the CD-induced power fading [5]. This observation is also evident from the subcarrier-BER distributions depicted in Figs. 5(c) and 5(d) for CDA-NODFTP-OFDM and CDA-NODFTP-FBMC with $\alpha = 0.844$, respectively. The

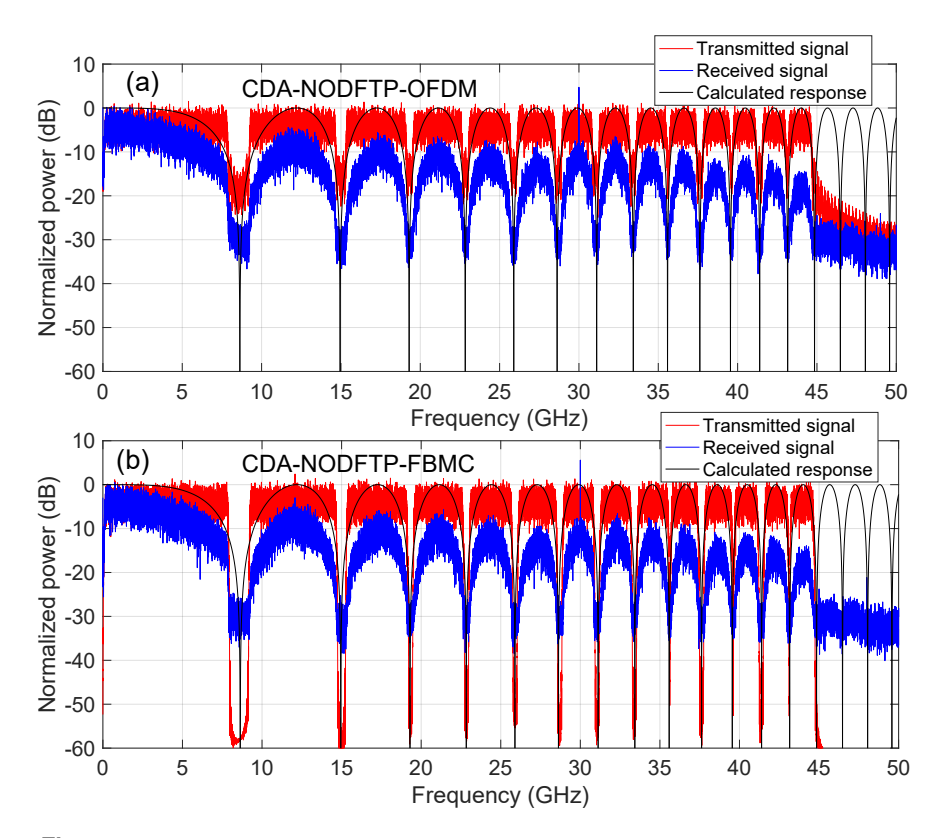


Fig. 4. Electrical spectra of transmitted and received (a) CDA-NODFTP-OFDM and (b) CDA-NODFTP-FBMC signals over a 50-km SSMF.

performance of fringe subcarriers in the CDA-NODFTP-OFDM system degrades similarly to that in a conventional DFTP-OFDM system [7]. Conversely, the CDA-NODFTP-FBMC exhibits less sensitivity to inter-symbol interference (ISI), even without CP, resulting in a more uniform subcarrier-BER distribution.

The pre-lookup table for determining the optimal compression factor, associated with transmission distance, can be established through offline simulation in practical applications, thereby eliminating the need for precise feedback of CSI. To validate its feasibility, a CD-constrained IM/DD channel with power fading is chosen. The primary impairment of the IM/DD system, which is CD-induced power fading, is considered in simulation while disregarding bandwidth limitations and nonlinear distortions. The simulation model can be expressed as r(k) = x(k) * h(k) + z(k) [5], where r(k) and x(k) represent the transmitted and received signals, respectively, z(k) denotes the additive white Gaussian noise (AWGN), set to 15 dB, and h(k) represents the transmission channel in discrete time domain with a normalized frequency response of $\cos(2\pi^2\beta_2 Lf^2)$. The fiber length L and dispersion coefficient D are 50 km and 16.75 ps/ns/km, respectively, while the remaining simulation parameters remain the same as those in the experiment. Figures 6(a) and 6(b) depict the BER as a function of compression factor for CDA-NODFTP-OFDM and CDA-NODFTP-FBMC in a simulated 50-km SSMF channel, respectively. The proposed CDA-NODFTP scheme is validated by achieving saturated BER performance with compression factors ranging from 0.802 (0.823) to 0.844 (0.844) for CDA-NODFTP-OFDM (CDA-NODFTP-FBMC), which is well matched the experimental results. Therefore, a optimal compression factor of 0.844 is chosen to achieve saturated BER performance in the experiment for both CDA-NODFTP-OFDM and CDA-NODFTP-FBMC.

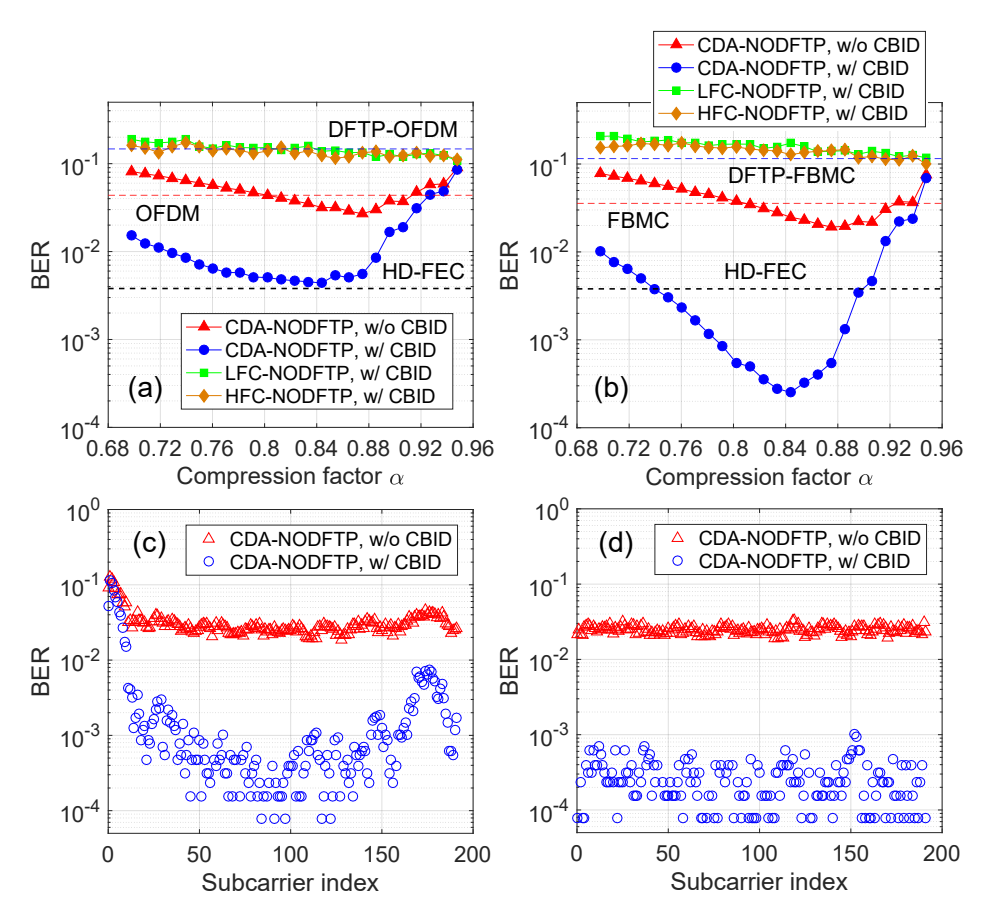


Fig. 5. BER versus compression factor for (a) CDA-NODFTP-OFDM and (b) CDA-NODFTP-FBMC. Subcarrier-BER distributions for (c) CDA-NODFTP-OFDM and (d) CDA-NODFTP-FBMC with α = 0.844. The results are measured after 50-km SSMF transmission at a ROP of 6 dBm.

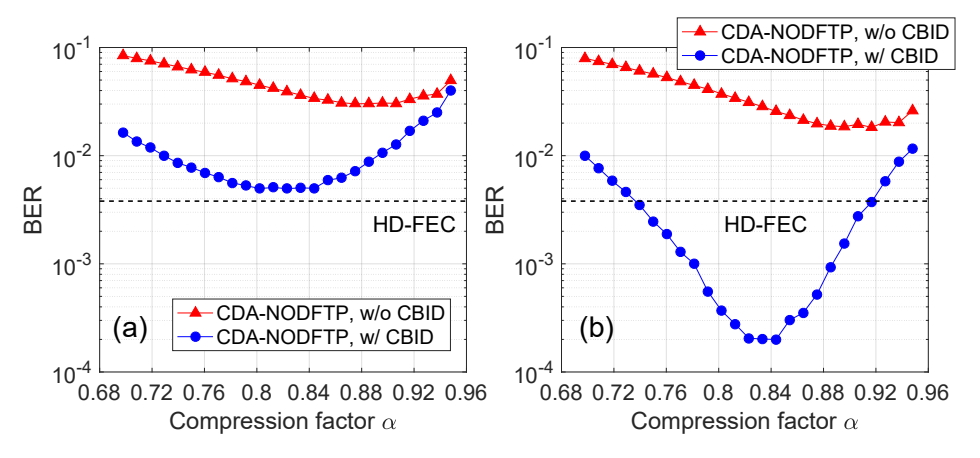


Fig. 6. BER versus compression factor for (a) CDA-NODFTP-OFDM and (b) CDA-NODFTP-FBMC in a simulated 50-km SSMF channel subject to CD-induced power fading.

The impact of the number of iterations of CBID algorithm on the BER performance is also investigated for the proposed CDA-NODFTP scheme. Figure 7 illustrates the BER performance under different numbers of iterations of the CBID algorithm for CDA-NODFTP-OFDM and CDA-NODFTP-FBMC transmissions after 50-km SSMF transmission at a ROP of 6 dBm. It is clear that the BERs of both NODFTP-OFDM and CDA-NODFTP-FBMC improve with an increase in the number of iterations. The performance improvement becomes negligible when the number of iterations exceeds 12. To strike a balance between performance and complexity, the number of iterations ν of the CBID algorithm is set to 12.

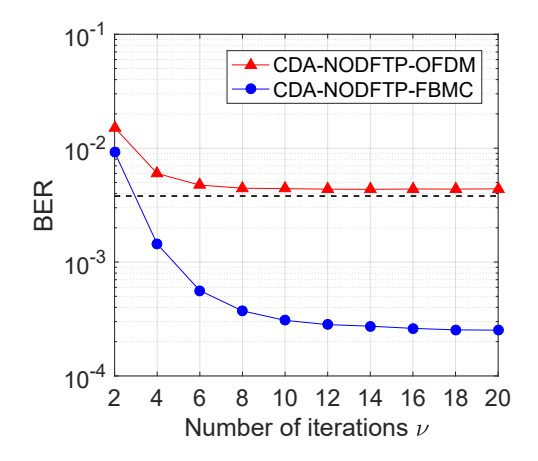


Fig. 7. BER versus the number of iterations ν of the CBID algorithm for CDA-NODFTP scheme after 50-km SSMF transmission at a ROP of 6 dBm.

Finally, the system transmission performance is evaluated and compared between the proposed CDA-NODFTP scheme and conventional multicarrier transmission schemes. Figure 8 shows the BER versus ROP for 90-Gb/s QPSK transmission using different schemes over a 50-km SSMF. One can see that the proposed CDA-NODFTP scheme effectively reduces the BERs of (DFTP-) OFDM and (DFTP-) FBMC signals by approximately one and two orders of magnitude, respectively. Furthermore, compared with CDA-NODFTP-OFDM, the CDA-NODFTP-FBMC with a well-localized prototype filter in both time and frequency domains can improve the receiver sensitivity by more than 3 dB, at the 7% HD-FEC BER limit of 3.8×10^{-3} .

The proposed CDA-NODFTP scheme is also assessed by conducting a performance comparison with the ABPL scheme [6], utilizing FBMC signals that exhibit better robustness against CDinduced power fading [5]. Figure 9(a) presents the BER as a function of ROP for CDA-NODFTPand ABPL-based FBMC signals at 90 Gb/s after 50-km SSMF transmission. The ABPL employs two bit-loading profiles, as illustrated in Fig. 9(b), based on the subcarrier-SNR distributions obtained through the CSI feedback and the prior information of accumulated CD (obtained by using the abovementioned simulation model) depicted in Figs. 9(c) and 9(d), respectively, at a ROP of 6 dBm. Note that the bit-loading profile for ABPL based on CSI feedback is dynamically updated with variations in ROP, while the bit-loading profile based on accumulated CD remains unchanged. It can be observed from Figs. 9(a)-9(d) that: (1) The CSI feedback ensures that the received subcarrier-SNR distribution of ABPL is aligned with the bit loading profile, thereby achieving the lowest BER among the three compared scenarios. (2) The ABPL can achieve an approximately 2.3-dB improvement in receiver sensitivity compared to the proposed CDA-NODFTP scheme, at the expense of requiring CSI feedback. (3) When switching from the feedback subcarrier-SNR distribution to the accumulated-CD based subcarrier-SNR distribution for ABPL, there is a mismatch between the received subcarrier-SNR distribution and the bit loading profile, which leads to a significant degradation in BER performance. (4) The proposed

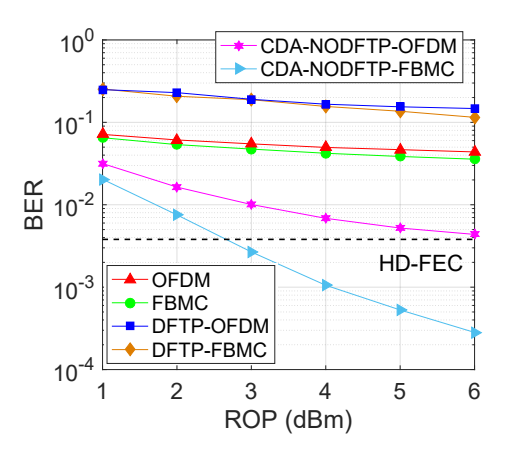


Fig. 8. BER versus ROP using different transmission schemes with a data rate of 90 Gb/s after 50-km SSMF transmission.

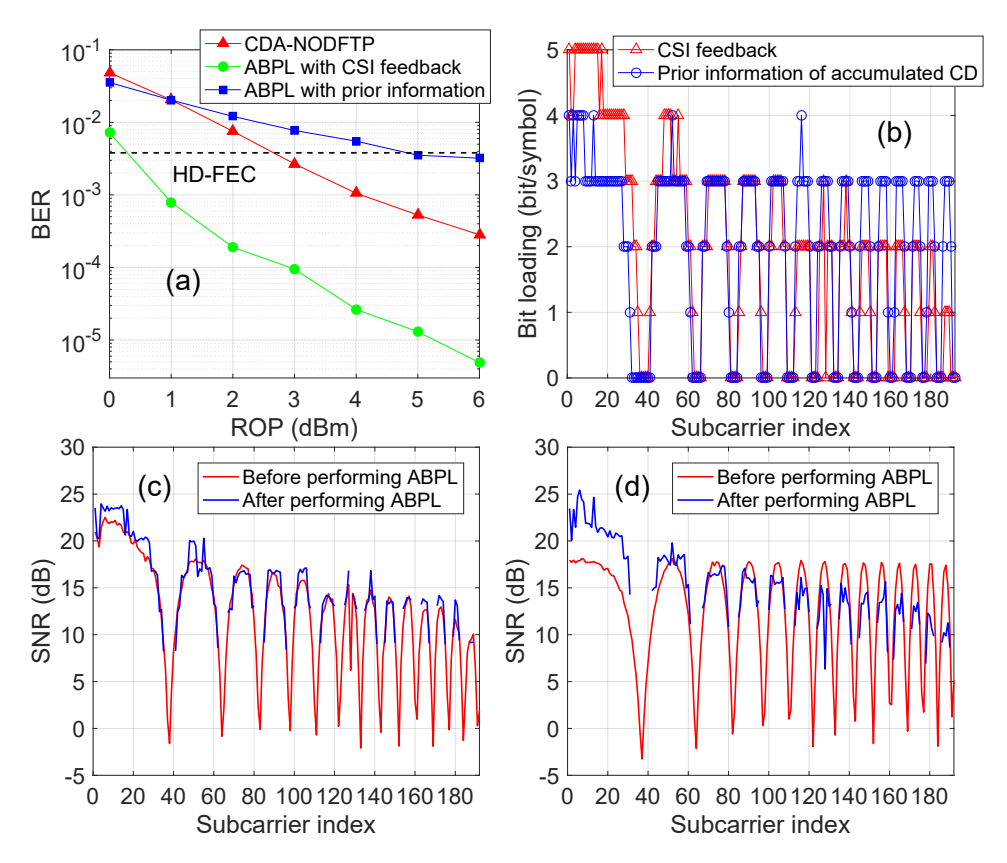


Fig. 9. (a) BER versus ROP using CDA-NODFTP and ABPL schemes for FBMC signals at 90 Gb/s after 50-km SSMF transmission. (b) Bit loading profiles at a ROP of 6 dBm. Subcarrier-SNR distributions before and after performing ABPL based on (c) CSI feedback and (d) prior information of accumulated CD at a ROP of 6 dBm.

CDA-NODFTP scheme exhibits superior performance compared to ABPL using CD response only, resulting in an approximately 2.1-dB improvement in receiver sensitivity, with the achieved BER under the 7% HD-FEC limit of 3.8×10^{-3} .

5. Conclusion

In this paper, we have proposed and experimentally demonstrated a CDA-NODFTP scheme to enhance resistance against the CD-induced power fading in a C-band 90-Gb/s IM/DD multicarriersignal transmission system over a 50-km dispersion-uncompensated link. Based on the prior knowledge of the dispersive channel, the CDA-NODFTP can flexibly keep the multicarrier signals' electrical spectra away from the CD-induced spectral nulls without sacrificing SE. Experimental results show that the BERs of multicarrier signals, both with and without conventional DFTP/ NODFTP, are above 0.03 due to the severe CD-induced power fading, making them unsuitable for data transmission. While the proposed CDA-NODFTP significantly improves the transmission performance of OFDM and FBMC signals, achieving reductions in BER by approximately one and two orders of magnitude, respectively. Compared with CDA-NODFTP-OFDM, the CDA-NODFTP-FBMC with a well-localized prototype filter in both time and frequency domains can achieve a more than 3-dB improvement in receiver sensitivity. Meanwhile, the CDA-NODFTP-FBMC exhibits superior performance compared to ABPL-FBMC using CD response only, resulting in an approximately 2.1-dB improvement in receiver sensitivity. Therefore, the proposed CDA-NODFTP scheme is promising to be applied in high-speed optical IM/DD multicarrier transmission systems, particularly for FBMC system.

Funding. National Natural Science Foundation of China (62101602); The Hong Kong Government General Research Fund (PolyU 15227321); PolyU Postdoc Matching Fund Scheme of the Hong Kong Polytechnic University (1-W150); Natural Science Foundation of Guangdong Province (2023A1515110666).

Disclosures. The authors declare no conflicts of interest.

Data availability. Data underlying the results presented in this paper are not publicly available at this time but may be obtained from the authors upon reasonable request.

References

- 1. X. Pang, O. Ozolins, R. Lin, *et al.*, "200 Gbps/Lane IM/DD Technologies for Short Reach Optical Interconnects," J. Lightwave Technol. **38**(2), 492–503 (2020).
- 2. M. Chagnon, "Optical Communications for Short Reach," J. Lightwave Technol. 37(8), 1779–1797 (2019).
- R. Rath, D. Clausen, S. Ohlendorf, et al., "Tomlinson–Harashima Precoding For Dispersion Uncompensated PAM-4 Transmission With Direct-Detection," J. Lightwave Technol. 35(18), 3909–3917 (2017).
- J. Zhang, H. Tan, L. Lu, et al., "Receive-diversity-aided power-fading compensation for C-band IM/DD OFDM systems," Opt. Lett. 48(9), 2237–2240 (2023).
- J. Zhang, H. Tan, L. Lu, et al., "Comparison of FBMC and OFDM with Adaptive Bit and Power Loading for CD-Constrained IM/DD Transmission over 50-km SSMF," J. Lightwave Technol. 42(8), 2702–2710 (2024).
- P. S. Chow, J. M. Cioffi, and J. A. C. Bingham, "A practical discrete multitone transceiver loading algorithm for data transmission over spectrally shaped channels," IEEE Trans. Commun. 43(2/3/4), 773–775 (1995).
- M. Chen, L. Wang, D. Xi, et al., "Comparison of Different Precoding Techniques for Unbalanced Impairments Compensation in Short-Reach DMT Transmission Systems," J. Lightwave Technol. 38(22), 6202–6213 (2020).
- M. Chen, A. Deng, L. Zhang, et al., "Precoding-Enabled FBMC/OQAM for Short-Reach IMDD Transmission," IEEE Photonics Technol. Lett. 33(23), 1305–1308 (2021).
- P. Song, Y. D. Z Hu, and C. Chan, "Nonlinear Distortion Mitigation with Non-Orthogonal DFT-precoding for DML-Based OFDM Optical Systems," in OFC W2A.30 (2023).
- 10. P. Song, Z. Hu, Y. Dai, et al., "Nonlinear distortion mitigation of DML-based OFDM optical systems with non-orthogonal DFT-precoding," Opt. Lett. 48(17), 4613–4616 (2023).
- Z. Li, W. Wang, D. Zou, et al., "DFT Spread Spectrally Efficient Frequency Division Multiplexing for IM-DD Transmission in C-Band," J. Lightwave Technol. 38(13), 3526–3532 (2020).
- 12. I. Darwazeh, T. Xu, T. Gui, et al., "Optical SEFDM system; bandwidth saving using non-orthogonal sub-carriers," IEEE Photonics Technol. Lett. 26(4), 3432–3437 (2014).
- J. Huang, Q. Sui, Z. Li, et al., "Experimental Demonstration of 16-QAM DD-SEFDM With Cascaded BPSK Iterative Detection," IEEE Photonics J. 8(3), 1–9 (2016).
- A. Sahin, I. Guvenc, and H. Arslan, "A survey on multicarrier communications: Prototype filters, lattice structures, and implementation aspects," IEEE Commun. Surv. Tutorials 16(3), 1312–1338 (2014).